# Real-Time On-Ramp Merging Control of Connected and Automated Vehicles using Pseudospectral Convex Optimization

Yang Shi[1], Zhenbo Wang[1], Tim J. LaClair[2], Chieh (Ross) Wang[2], and Jinghui Yuan[2]

***Abstract*— Highway on-ramp merging can be a challenging task for human drivers due to the complex vehicle negotiations and interactions in limited time and space. Connected and automated vehicles (CAVs) have great potential to address the problem and offer many benefits in terms of safety, traffic efficiency, and fuel economy. However, real-time optimal control of CAVs still faces many challenges, including nonlinear dynamics, complex inter-vehicle interactions, and a highly dynamic and uncertain traffic environment. To address these challenges, we develop a novel control approach that balances the solution optimality and computational efficiency to determine optimal merging speed profiles in real time. Specifically, by employing a pseudospectral method and a sequential convex programming approach, two algorithms are proposed and implemented within the model predictive control (MPC) framework to enable real-time generation of optimal solutions for potential on-vehicle applications. The convergence and optimality of the proposed algorithms are validated by comparing with a general-purpose solver under different traffic scenarios.**

## I. INTRODUCTION

The latest developments in connected and automated vehicles (CAVs) have opened up new opportunities for the revolution of future transportation systems. The U.S. Department of Transportation is actively preparing to lead the advance in CAV technologies, and four main potential benefits of introducing CAVs to transportation systems have been spotlighted [1]: road safety, economic and societal benefits, efficiency and convenience, and public mobility. A number of studies have been conducted to investigate the challenges and opportunities involving CAVs [2], [3], [4].

According to the National Highway Traffic Safety Administration (NHTSA), motor vehicle crash fatalities are higher on urban highways compared to rural roads since 2016. As a comparison, urban fatalities increased 48% since 2011 and the rural fatalities decreased by 6.2%. In 2020, the number of urban fatalities is 30% higher than the rural areas [5]. As one of the most challenging scenarios on urban highways, on-ramp merging has attracted wide attention from many researchers. The merging process involves complex vehicle negotiations and interactions, and drivers have to perform situation assessment, decision-making, and vehicle operations within a limited distance and time. One of the conventional methods to improve merging safety is ramp metering [6]. However, ramp metering suffers disadvantages such as increased travel delay and emissions [7].

On-ramp merging aims to coordinate the vehicles on the mainline and the ramp to pass through the merging area safely and as smoothly as possible. In the CAV environment, vehicles are able to communicate with each other (V2V) and with the infrastructure (V2I) about their current and planned trajectories (position, speed and acceleration) and other information, with which the vehicles can be coordinated to make smooth merging maneuvers for safety, mobility, and fuel efficiency purposes. Many studies have demonstrated that trajectory optimization of vehicles can reduce travel time and fuel consumption, increase throughput, and improve safety [8], [9], [10]. The basic idea is to find or create a suitable gap between mainline vehicles for the on-ramp vehicles to merge, and to avoid or minimize the braking caused by the merging maneuver. However, most existing approaches are not suitable for real-time implementation due to high computational cost and and inability to cope with non-convex motion constraints and dynamic environments.

In this paper, we develop a new merging control framework that balances the solution optimality and computational efficiency with guaranteed merging safety. Specifically, a pseudospectral convex optimization formulation is proposed for the merging of CAVs at highway on-ramps. In addition, the proposed algorithm is combined with the model predictive control (MPC) strategies to cope with uncertainties and improve inter-vehicle coordination.

## II. PROBLEM FORMULATION

The goal of this study is to develop an optimal speed control model that minimizes fuel consumption, avoids collision, and reduces congestion for CAVs merging at highway on-ramps. As shown in Fig. 1, a typical single lane highway merging scenario is considered. After entering a control zone, CAVs are assigned a target traveling speed by the centralized controller. Then, the speed profiles are computed in real-time by each vehicle to regulate its movement with minimum acceleration/deceleration maneuvers. We assume that the planned speed trajectories of all vehicles in the control zone are available to other vehicles through V2V communication. This section details the vehicle dynamic model and the formulation of the speed optimization problem.

This manuscript has been authored in part by UT-Battelle LLC under contract DE-AC05-00OR22725 with the US Department of Energy (DOE). The US government retains and the publisher, by accepting the article for publication, acknowledges that the US government retains a nonexclusive, paid-up, irrevocable, worldwide license to publish or reproduce the published form of this manuscript, or allow others to do so, for US government purposes. DOE will provide public access to these results of federally sponsored research in accordance with the DOE Public Access Plan (http://energy.gov/downloads/doe-public-access-plan).

[1]Y. Shi and Z. Wang are with the Department of Mechanical, Aerospace, and Biomedical Engineering, University of Tennessee, Knoxville, TN 37996, USA: yshi38@vols.utk.edu; zwang124@utk.edu [2]T. J. LaClair, C. Wang, and J. Yuan are with the Buildings and Transportation Science Division, Oak Ridge National Laboratory, Oak Ridge, TN 37831, USA: laclairtj@ornl.gov; cwang@ornl.gov; yuanj@ornl.gov.

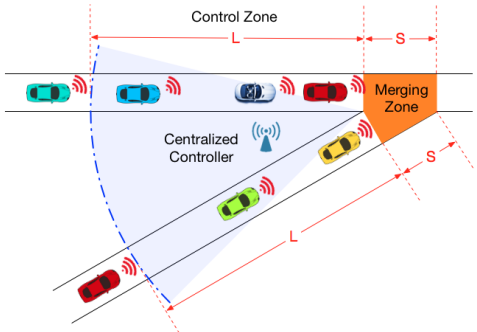


Fig. 1. Schematic of CAV-based on-ramp merging.

### A. Vehicle Dynamics

In this paper, the longitudinal dynamics of the vehicle are considered as [11]:

$$m\dot{v} = \frac{T_\mathrm{e}}{r_\mathrm{g}} - F_\mathrm{b} - F_\mathrm{aero} - F_\mathrm{m} \tag{1}$$

with mass $m$, velocity $v$, and engine torque $T_\mathrm{e}$. The term $r_\mathrm{g}$ is defined as the wheel radius divided by total gear ratio and is assumed to be constant in this paper. $F_\mathrm{b}$ represents the braking force at the wheels, and $F_\mathrm{aero}$ is the force due to aerodynamic resistance, as given by:

$$F_\mathrm{aero} = \frac{1}{2}\rho A C_\mathrm{D} v^2, \tag{2}$$

where $C_\mathrm{D}$ is the aerodynamic drag coefficient, $A$ denotes the frontal area of the vehicle, and $\rho$ represents air density. $F_\mathrm{m}$ is the resistant force due to the road grade and rolling resistance, as given by:

$$F_\mathrm{m} = mg(\mu\cos\theta + \sin\theta), \tag{3}$$

where $g$ is the gravitational constant, $\mu$ denotes the rolling resistance coefficient, and $\sin\theta$ represents the road gradient, which is assumed to be constant in this paper.

The fuel consumption model is adopted from [12], where the fuel consumption rate $\dot{m}_\mathrm{f}$ is approximated by:

$$\dot{m}_\mathrm{f} = \begin{cases} \alpha_0 + \alpha_1 v + \alpha_2 v^2 + \alpha_3 v^3 \\ \quad +a(\beta_0 + \beta_1 v + \beta_2 v^2), & a > 0 \\ \alpha_0, & a \leqslant 0 \end{cases} \tag{4}$$

where $a$ is the vehicle's acceleration, $\alpha_i$ and $\beta_i$ are constants of the third order polynomial function determined by fitting the experiment data. When vehicles are braking or idling, the fuel consumption is a constant $\alpha_0$. The selected values of the above parameters are summarized in Table I.

TABLE I
PARAMETERS OF VEHICLE DYNAMICS.

| Parameter (Unit) | Value | Parameter (Unit) | Value |
|---|---|---|---|
| $m$ (kg) | 1200 | $u_\mathrm{e}^{\max}$ (m/s$^2$) | 3 |
| $\rho$ (kg/m$^3$) | 1.184 | $u_\mathrm{b}^{\max}$ (m/s$^2$) | 3 |
| $A$ (m$^2$) | 2.5 | $v^{\max}$ (m/s) | 20 |
| $C_\mathrm{D}$ | 0.32 | $v^{\min}$ (m/s) | 0 |
| $g$ (m/s$^2$) | 9.8 | $\mu$ | 0.015 |
| $\alpha_0$ (mL/s) | 0.1569 | $\beta_0$ (mL/s/m) | 0.07224 |
| $\alpha_1$ (mL/m) | 2.450e-2 | $\beta_1$ (mLs$^2$/m$^2$) | 9.681e-2 |
| $\alpha_2$ (mLs/m$^2$) | -7.415e-4 | $\beta_2$ (mLs$^3$/m$^3$) | 1.075e-3 |
| $\alpha_3$ (mLs$^2$/m$^3$) | 5.975e-5 | $R_0$ (m) | 2.5 |
| $t_\mathrm{hd}$ ($s$) | 1.3 | | |

### B. Optimal Control Problem Formulation

In this paper, novel rules (see Fig. 2) are designed to determine the merging sequence considering different control goals for the vehicles on the mainline road and the on-ramp. To increase the road capacity and traffic efficiency, the on-ramp vehicles should avoid the "stop-and-go" pattern and merge to the mainline road at the earliest available gap. Meanwhile, the vehicles travelling on the mainline road should avoid sudden braking caused by the merging vehicles, which could lead to collisions, congestion and additional fuel consumption. Thus, when there are on-ramp vehicles seeking to merge, the mainline vehicles need to actively create gaps if acceleration is possible. In addition, when there is no conflict between mainline vehicles and on-ramp vehicles, they can both travel at the fuel-optimal speed.

After the merging sequence is determined, the arrival time of the newly detected vehicle to the merging zone is scheduled, and a target speed is calculated correspondingly. To summarize, Table II lists all the cases for calculating the arrival time to the merging zone. The calculation starts from the newly detected vehicle and passes forward or backward to the affected vehicles in the control zone. The arrival time of the preceding vehicle is denoted as $t_\mathrm{arrival}^\mathrm{front}$ and the arrival time of the following vehicle is $t_\mathrm{arrival}^\mathrm{back}$. $t_\mathrm{hd}$ is the time headway requirement for safety considerations. When no arrival time needs to be assigned, the vehicle can travel at the fuel-optimal speed or the same speed as the preceding vehicle.

Once the merging sequence and the arrival time are determined, a speed profile will be computed to guide the vehicles passing through the control zone. The optimal speed control is formulated as a nonlinear optimal control problem that minimizes cost functions for fulfilling multiple driving requirements, such as safe distance with the preceding vehicle, passenger comfort, and desired speed. Instead of imposing a terminal time to the problem, we convert the arrival time into a reference speed for the vehicle to track. As such, the speed profile can be generated iteratively over a short rolling time horizon. The problem is as follows:

**Problem 1**:

$$\underset{x,v,u}{\text{minimize}} J = \int_t^{t+T} \omega_2 R(t)^2 + \omega_3 (v - v_\mathrm{d})^2 + \omega_4 (u(t) - u_\mathrm{d}(t))^2 dt \tag{5}$$

$$s.t.\ \dot{x} = v \tag{6}$$

$$\dot{v} = u_\mathrm{e} - u_\mathrm{b} - \frac{\rho A C_\mathrm{D} v^2}{2m} - (\mu\cos\theta + \sin\theta)g \tag{7}$$

$$u_\mathrm{d}(t) = \frac{\rho A C_\mathrm{D} v^2}{2m} - (\mu\cos\theta + \sin\theta)g \tag{8}$$

$$R(t) = R_0 + v t_\mathrm{hd} + x - x_\mathrm{p} \tag{9}$$

$$x_\mathrm{p} - x \geqslant R_0 \tag{10}$$

$$0 \leqslant u_\mathrm{e} \leqslant u_\mathrm{e}^{\max} \tag{11}$$

$$0 \leqslant u_\mathrm{b} \leqslant u_\mathrm{b}^{\max} \tag{12}$$

$$d^{\min} \leqslant v \leqslant v^{\max} \tag{13}$$

In this problem, the control inputs $u$ include the vehicle's acceleration $u_\mathrm{e}$ and deceleration $u_\mathrm{d}$. The first term of the

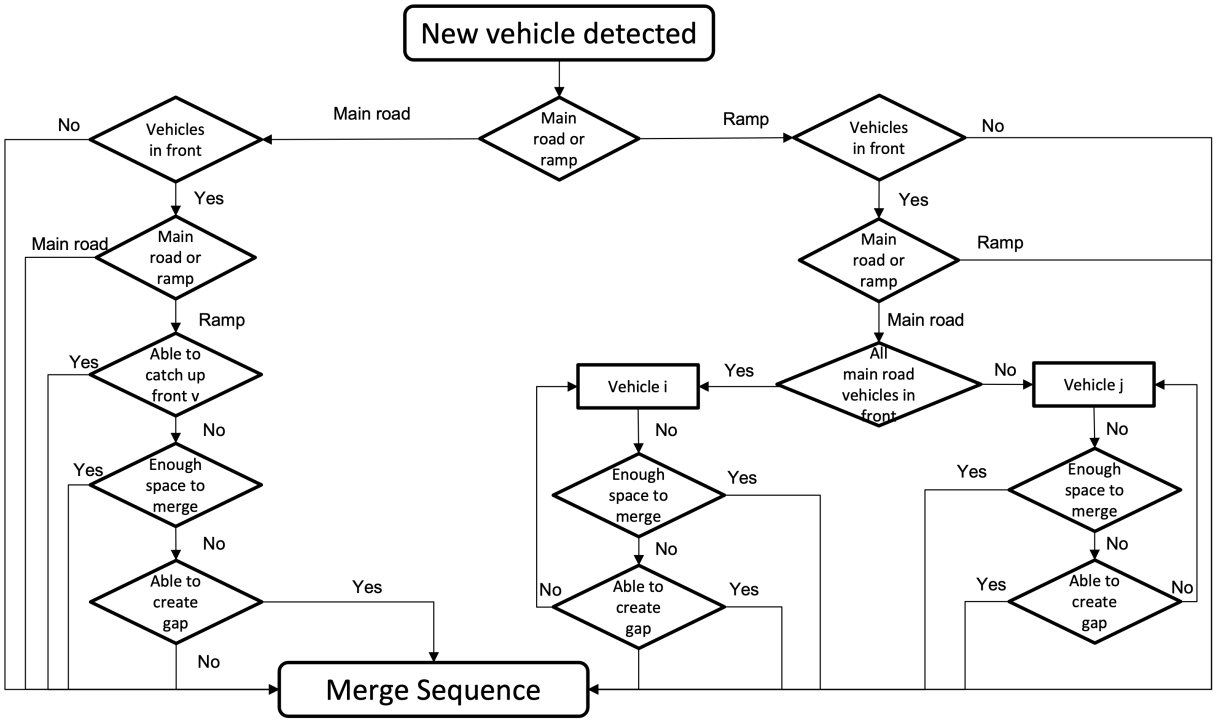


Fig. 2. A rule-based cooperative merging strategy.

TABLE II

LIST OF CASES FOR CALCULATING THE ARRIVAL TIME TO THE MERGING ZONE.

| Vehicle | Case | Arrival time |
|---|---|---|
| mainline | 1: no need or not able to accelerate | — |
| | 2: need to accelerate to catch up to preceding vehicle | $t_{\text{arrival}}^{\text{front}} + t_{\text{hd}}$ |
| | 3: need to accelerate to make a gap | $t_{\text{arrival}}^{\text{back}} - t_{\text{hd}}$ |
| Ramp | 1: no need or not able to accelerate | — |
| | 2: accelerate to merge into a gap without adjustment of the mainline vehicles | $t_{\text{arrival}}^{\text{front}} + t_{\text{hd}}$ |
| | 3: accelerate to merge into a gap created by acceleration of the mainline vehicles | $t_{\text{arrival}}^{\text{back}} - t_{\text{hd}}$ |
| | 4: accelerate to merge together with the preceding on-ramp vehicle without adjustment of the mainline vehicles | $t_{\text{arrival}}^{\text{front}} + t_{\text{hd}}$ |
| | 5: accelerate to merge into a gap created by acceleration of the mainline vehicles together with the preceding on-ramp vehicle | $t_{\text{arrival}}^{\text{back}} - t_{\text{hd}}$ |

cost functional $J$ is to keep a safe distance with the preceding vehicle. $R$ is the deviation from this safety distance and given by Eq. (9), where $R_0$ is the minimum safe distance between the vehicles, $t_{\text{hd}}$ is the headway requirement measured in time, and $x_{\text{p}}$ is the position of the preceding vehicle. The second term of $J$ is to make sure that the vehicle tracks the desired traveling speed. The last term of $J$ is a penalty for reducing control efforts and avoiding jitters. Since the vehicles need to consume fuel to maintain speed, a compensation value $u_{\text{d}}(t)$ is included for better optimization performance. Each term is multiplied by an adjustable weight to facilitate behavioral decision-making. The weight $\omega_2$ for maintaining inter-vehicle distance is defined as $\omega_2 = \gamma e^{\alpha(x-x_{\text{p}})}$ [13], where $\gamma$ and $\alpha$ are adjustable parameters. When the vehicle is close to the preceding vehicle, $\omega_2$ grows exponentially to avoid collision. While the relative distance between vehicles exceeds the desired value, the whole penalty term will increase, such that the vehicles can maintain a small gap for better fuel efficiency and traffic mobility. When the preceding vehicle is far away, $\omega_2$ becomes negligibly small. Constraints in Eqs. (11) to (13) define the lower and upper bounds of the control variables and the speed range of the vehicle.

The goal of Problem 1 is to track a reference velocity while keeping a safe distance with the preceding vehicle and having comfort driving maneuvers. The reference velocity $v_{\text{d}}$ is computed as the distance to the merging zone divided by the scheduled arrival time. If the vehicle is not assigned with an arrival time, it can use the fuel-optimal speed or the same speed as the preceding vehicle, depending on which one is smaller. In addition, based on the fuel consumption model in Eq. (4), the optimal cruising speed $v^*$ can be obtained at the minimum fuel consumption rate per unit distance as a solution of

$$\frac{d}{dv}\left(\frac{\dot{m}}{v}\right) = -\frac{\alpha_0}{v^2} + 2\alpha_3 v + \alpha_2 = 0. \tag{14}$$

## III. Optimal Control Method

Problem 1 is a nonconvex optimal control problem due to the nonlinear dynamics and the nonconvex terms in the cost functional. To allow optimal solutions in real time, we develop a pseudospectral convex optimization method for the considered merging control problem. Specifically, the pseudospectral method is used to discretize the problem, and then the nonconvex structures are transformed into tractable formulations to find approximate optimal solutions using sequential convex programming (SCP).

To formulate a convex optimization problem, the equality constraint functions in Problem 1 must be affine. In particular, the nonlinear terms in Eq. (7) need to be linearized by a first-order Taylor series expansion with respect to a reference speed trajectory, $v^{k-1}(t)$, which is the solution of the previous SCP iteration. The successive linearized dynamics for the $k$-th iteration are as follows:

$$\dot{v} \approx \frac{\rho A C_{\mathrm{D}}}{2m}((v^{k-1})^2 - 2v^{k-1}v) - (\mu\cos\theta + \sin\theta)g \quad (15)$$

Similarly, the nonlinear term $u_{\mathrm{d}}$ in Eq. (8) can also be linearized about the previous solution $v^{k-1}(t)$ as follows:

$$u_{\mathrm{d}}(t) \approx \frac{\rho A C_{\mathrm{D}}}{2m}(2v^{k-1}v - (v^{k-1})^2) + (\mu\cos\theta + \sin\theta)g \quad (16)$$

With the above successive linearizations, Problem 1 was converted into the following convex optimal control problem:

**Problem 2**:

$$\begin{aligned} &\underset{x,v,u}{\text{minimize}} \quad \text{Eq. (5)} \\ &\text{subject to} \quad \text{Eq. (6), Eq. (9), Eq. (10), Eq. (11),} \\ &\text{Eq. (12), Eq. (13) Eq. (15), and Eq. (16).} \end{aligned}$$

Two algorithms were developed to obtain an approximate optimal solution to Problem 1 by solving a sequence of Problem 2 with discretized state variables.

**Algorithm 1: Line-search SCP**:

1) Set $k = 0$. Generate an initial vehicle trajectory $\hat{\boldsymbol{z}}^0$ for the solution procedure by propagating the equation of motion in Eqs. (6) and (7) with a specific constant control from the current state of the vehicle, $x(t_0) = x_0$ and $v(t_0) = v_0$. Set $k = k + 1$.

2) For $k \geqslant 1$, parameterize Problem 2 using $\hat{\boldsymbol{z}}^{k-1}$, solve Problem 2 for a solution $\boldsymbol{z}^k = \{x^k, v^k, u^k\}$.

3) Check the convergence criteria:

$$\begin{cases} \sup\limits_{t_0 \leqslant t \leqslant t_{\mathrm{f}}} \left|x^k - x^{k-1}\right| \leqslant \epsilon_1 \\ \sup\limits_{t_0 \leqslant t \leqslant t_{\mathrm{f}}} \left|v^k - v^{k-1}\right| \leqslant \epsilon_2 \end{cases}, \ k > 1 \quad (17)$$

where $\epsilon_1$ and $\epsilon_2$ are prescribed tolerances for the convergence criteria. If the above criteria are satisfied, the algorithm goes to step 5; otherwise to step 4.

4) Compute the search direction $\boldsymbol{p}^k = \boldsymbol{z}^k - \hat{\boldsymbol{z}}^{k-1}$ for the next iteration. Find a suitable step length $\alpha^k$ by starting from $\alpha^0 = 1$ and decreasing it with a contraction factor $c_1$, such that $\alpha^k = c_1\alpha^{k-1}$, until sufficient decrease in the objective functional $J$ is achieved with a specified constant $c_2$, as described by the following inequality :

$$\begin{cases} J(\boldsymbol{z}^k + \alpha^k\boldsymbol{p}^k) & \geqslant J(\boldsymbol{z}^k) + (1-c_2)\alpha^k\nabla J_k^T\boldsymbol{p}^k \\ J(\boldsymbol{z}^k + \alpha^k\boldsymbol{p}^k) & \leqslant J(\boldsymbol{z}^k) + c_2\alpha^k\nabla J_k^T\boldsymbol{p}^k \end{cases} \quad (18)$$

$$\text{subject to} \quad 0 < c_2 < 1/2 \quad (19)$$

Then, update the reference trajectory $\hat{\boldsymbol{z}}^k = \hat{\boldsymbol{z}}^{k-1} + \alpha^k\boldsymbol{p}^k$, set $k = k + 1$, and go back to step 2.

5) The iteration is terminated and a solution is found as $\boldsymbol{z}^* = \{x^*, v^*, u^*\} = \{x^k, v^k, u^k\}$.

Step 4 of Algorithm 1 is a line-search algorithm used to find a feasible search step that facilitates stable convergence of the SCP. In addition, the inequality condition in Eq. (18) is called the Goldstein condition, which ensures that the step length, $\alpha^k$, generates a sufficient but not too small decrease in the cost function [14, p. 36].

An alternative approach proposed in this paper is based on trust-region methods, which have the same purpose of improving the convergence of SCP as line-search methods. Trust-region methods first define a trustworthy region around the initial guess then compute the step as an approximate solution in this region. If the step does not meet the criteria, the size of the trust-region is reduced and another iteration is performed. If the step makes sufficient progress, the trust-region radius can be enlarged or remains the same. In this paper, a trust-region SCP method is designed for the considered speed control problem as follows.

**Algorithm 2: Trust-region SCP**:

1) Set $k = 0$. Generate an initial vehicle trajectory $\hat{\boldsymbol{z}}^0$ for the solution procedure by propagating the equation of motion in Eqs. (6) and (7) with a specific constant control from the current state of the vehicle, $x(t_0) = x_0$ and $v(t_0) = v_0$. Select appropriate values for trust-region radius $\delta = \delta_0$ and constants $0 < \eta < \beta_1 < 1 < \beta_2$. Set $k = k + 1$.

2) For $k \geqslant 1$, parameterize Problem 2 using $\hat{\boldsymbol{z}}^{k-1}$, solve Problem 2 subject to the trust-region constraint Eq. (20) for a solution $\boldsymbol{z}^k = \{x^k, v^k, u^k\}$.

$$|\boldsymbol{z}^k - \hat{\boldsymbol{z}}^{k-1}| \leqslant \delta \quad (20)$$

3) Check the convergence criteria:

$$\begin{cases} \sup\limits_{t_0 \leqslant t \leqslant t_{\mathrm{f}}} \left|x^k - x^{k-1}\right| \leqslant \epsilon_1 \\ \sup\limits_{t_0 \leqslant t \leqslant t_{\mathrm{f}}} \left|v^k - v^{k-1}\right| \leqslant \epsilon_2 \end{cases}, \ k > 1 \quad (21)$$

where $\epsilon_1$ and $\epsilon_2$ are prescribed tolerances for the convergence criteria. If the above criteria are satisfied, the algorithm goes to step 5; otherwise to step 4.

4) Use $\boldsymbol{z}^k$ to compute the model ratio $\nu^k$ as:

$$\nu^k = \frac{J(\hat{\boldsymbol{z}}^{k-1}) - J(\boldsymbol{z}^k)}{J(\hat{\boldsymbol{z}}^{k-1}) - J'(\boldsymbol{z}^k)} \quad (22)$$

where $J(\boldsymbol{z}^k)$ is the original objective functional defined in Eq. (5) with nonlinear dynamics, and $J'(\boldsymbol{z}^k)$ is the parameterized objective functional with linearized dynamics. The model ratio is a quality measurement of the approximate

solution, in which the numerator of Eq. (22) is the actual reduction of the objective functional, and the denominator is the predicted reduction of the objective functional. If $\nu^k < 0.25$, then the trust-region radius $\delta$ is reduced such that $\delta = \beta_1\delta$; if $\nu^k > 0.75$, $\delta$ is enlarged by $\delta = \beta_2\delta$; otherwise, $\delta$ remains the same. Next, if $\nu^k > \eta$, then update the reference trajectory $\hat{\boldsymbol{z}}^k = \boldsymbol{z}^k$, set $k = k+1$, and go back to step 2; otherwise, discard the solution $\boldsymbol{z}^k$, and go back to step 2 to resolve Problem 2.

5) The iteration is terminated and solution is found as $\boldsymbol{z}^* = \{x^*, v^*, u^*\} = \{x^k, v^k, u^k\}$.

Step 4 is the process of finding a suitable trust-region radius for the next iteration. The size of the trust-region $\delta$ is critical to the speed of convergence. When $\delta$ is too large, it is unlikely to find a step that is close to the optimal solution. If $\delta$ is too small, it may take many extra iterations to reach the optimal solution. Detailed discussion of the trust-region methods can be found in [14, p. 66]. Compared to the line-search method in Algorithm 1, the trust-region method does not need to calculate the derivative of the objective functional $J$, such that the computation cost could be reduced. However, in some cases, it may take more iterations to converge due to the large model errors or strong artificial infeasibility.

Furthermore, the developed SCP algorithms were implemented under an MPC framework. MPC solves the control problem over a fixed time horizon and only applies a short interval of the control solution to the vehicle [15]. The proposed convex optimization-based real-time speed control framework consists of three major components: 1) MPC that enables online control with instant response to the environment, 2) Pseudospectral discretization that improves the accuracy and convergence of the numerical optimization algorithms, and 3) Convex optimization that enables real-time computation. At each time step, the algorithm produces the control commands and the predicted trajectory for each vehicle in the control zone. After the execution of the control commands, the new states and predicted trajectories are shared with other vehicles via V2V communications. Then, a new iteration is performed in the next time step.

## IV. Simulation Results

In this section, a series of simulation results are presented to demonstrate the effectiveness and performance of the proposed on-ramp merging method. The optimization algorithms were implemented in YALMIP [16]. The convex solver was Gurobi [17], and the nonlinear optimization solver used for comparison was IPOPT [18].

In the following simulations, all vehicles are considered to be identical with the same parameters listed in Table I. The slopes for highway and ramp are assumed to be constant at 0%. The fuel-optimal speed is $v^* = 13.46$ m/s obtained by solving Eq. (14). The maximum speed limit of the highway is set to $v^{\max} = 30$ m/s, while the minimum allowable speed is $v^{\min} = 0$ m/s.

### A. Convergence Analysis

First, we considered a simple example where an on-ramp vehicle travels 400 m to merge at $t = 20$ s. As shown in Fig. 3, the blue and green lines with markers are the trajectories computed by Algorithm 1 and 2, respectively. The red lines are the baseline results from IPOPT. It can be seen from the comparison that the control profiles are in good agreement, which validates the optimality and accuracy of the solutions from the proposed SCP algorithms. In particular, the absolute errors of the terminal point were $1.27e-2$ m and $3.20e-5$ m/s for the position and velocity, respectively. The convergence of the SCP algorithms is displayed in Fig. 4. The convergence tolerances are set to $\epsilon_1 = 1e-6$ and $\epsilon_2 = 1e-6$. As shown in the figure, it takes 3 iterations to converge for both SCP algorithms. The convergence processes are very similar.

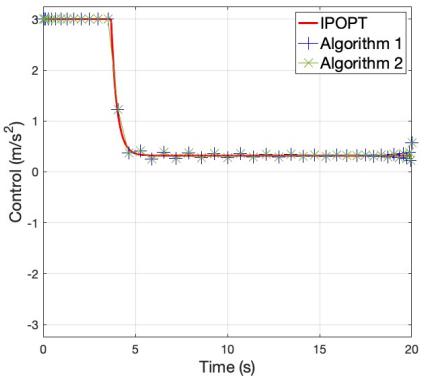

Fig. 3. Comparison of optimal control profiles.

In regard to the computational cost, it takes IPOPT about 127 s to solve for the baseline trajectory in MATLAB on a MacBook Pro with a 64-bit Mac OS and an Intel Core i7 2.2 GHz processor. In contrast, it costs Gurobi less than 0.1 s to solve Problem 2 at each iteration in the above example. Additionally, the CPU time cost of the SCP algorithms can be decreased for fewer discretization nodes or higher tolerances. The computational efficiency could be further improved if the algorithms are implemented in compiled programming environment or on a more powerful computation devices.

### B. Case Study: Coordination of 20 Vehicles

The SCP algorithm was then implemented within the MPC framework. The rolling time horizon of MPC was set to be 10 s. All the vehicles started from position 0 with a random initial speed ranging from 10 to 20 m/s. Each vehicle joined the simulation randomly with a probability based on the traffic volume. In this case, the traffic volume was 900 vehicles per hour with a probability of 25% for each second. The purpose of this case study was to validate that the proposed method was able to coordinate the merging process continuously. Fig. 5 displays 20 trajectories obtained by the proposed algorithms. It can be seen that all the vehicles enter the merging zone with a safe distance between each other. The results indicate that all the vehicles are able to travel at a fuel-optimal speed of 13.46 m/s without conflicts.

## V. Conclusion

In this paper, a CAV-based optimal speed control approach was developed for highway on-ramp merging with guaranteed safety, real-time performance, and high fuel efficiency.

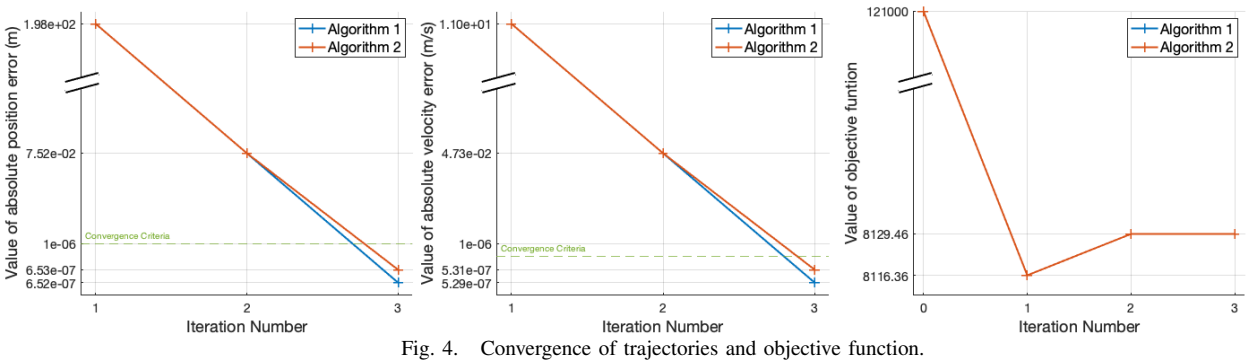


Fig. 4. Convergence of trajectories and objective function.

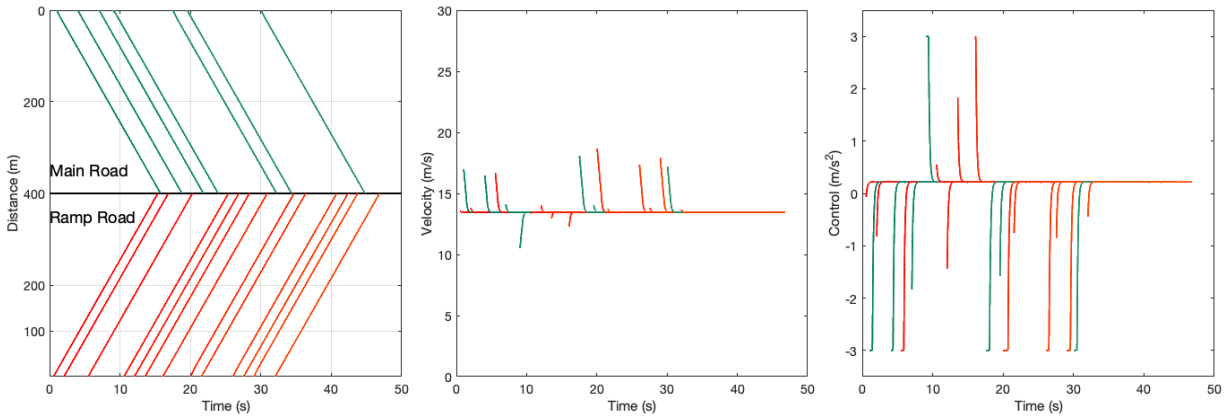


Fig. 5. Trajectories and control profiles under MPC framework.

Specifically, by leveraging the pseudospectral discretization method and the sequential convex programming method, the proposed algorithms had high computational efficiency that enables potential real-time applications. To avoid collision and improve inter-vehicle coordination, the safety distance constraint was considered in the problem formulation. In addition, the MPC framework was applied to perform the real-time update of maneuvers for instant response to dynamic traffic environments. The convergence and optimality of the proposed algorithms were validated by comparing with IPOPT under different traffic scenarios.

## REFERENCES


[1] US Department of Transportation, "Ensuring american leadership in automated vehicle technologies: Automated vehicles 4.0," *Technical report*, 2020.

[2] D. J. Fagnant and K. Kockelman, "Preparing a nation for autonomous vehicles: opportunities, barriers and policy recommendations," *Transportation Research Part A: Policy and Practice*, vol. 77, pp. 167–181, 2015.

[3] M. Taiebat, A. L. Brown, H. R. Safford, S. Qu, and M. Xu, "A review on energy, environmental, and sustainability implications of connected and automated vehicles," *Environmental Science & Technology*, vol. 52, no. 20, pp. 11 449–11 465, 2018.

[4] J. Guanetti, Y. Kim, and F. Borrelli, "Control of connected and automated vehicles: State of the art and future challenges," *Annual Reviews in Control*, vol. 45, pp. 18–40, 2018.

[5] N. H. T. S. Administration, "Overview of motor vehicle crashes in 2020," US Department of Transportation, Tech. Rep., 2020.

[6] A. Mizuta, K. Roberts, L. Jacobsen, and N. Thompson, "Ramp metering: A proven, cost-effective operational strategy," *US Department of Transportation Federal Highway Administration, Tech. Rep*, 2014.

[7] C. Systematics, "Twin cities ramp meter evaluation," Cambridge Systematics, Tech. Rep., 2001.

[8] J. Rios-Torres and A. A. Malikopoulos, "A survey on the coordination of connected and automated vehicles at intersections and merging at highway on-ramps," *IEEE Transactions on Intelligent Transportation Systems*, vol. 18, no. 5, pp. 1066–1077, 2016.

[9] J. Rios-Torres, Z. Khattak, J. Han, C. Wang, and H. Lim, "Assessing the implications of automated merging control in a mixed and heterogeneous traffic environment," in *2021 IEEE International Intelligent Transportation Systems Conference (ITSC)*, 2021, pp. 1098–1104.

[10] C. Letter and L. Elefteriadou, "Efficient control of fully automated connected vehicles at freeway merge segments," *Transportation Research Part C: Emerging Technologies*, vol. 80, pp. 190–205, 2017.

[11] A. Vahidi, A. Stefanopoulou, and H. Peng, "Recursive least squares with forgetting for online estimation of vehicle mass and road grade: theory and experiments," *Vehicle System Dynamics*, vol. 43, no. 1, pp. 31–55, 2005.

[12] M. A. S. Kamal, M. Mukai, J. Murata, and T. Kawabe, "Ecological vehicle control on roads with up-down slopes," *IEEE Transactions on Intelligent Transportation Systems*, vol. 12, no. 3, pp. 783–794, 2011.

[13] M. Kamal, M. Mukai, J. Murata, and T. Kawabe, "Ecological driver assistance system using model-based anticipation of vehicle–road–traffic information," *IET Intelligent Transport Systems*, vol. 4, no. 4, pp. 244–251, 2010.

[14] J. Nocedal and S. Wright, *Numerical optimization*. Springer Science & Business Media, 2006, pp. 36,66.

[15] E. F. Camacho and C. B. Alba, *Model predictive control*. Springer Science & Business Media, 2013.

[16] J. Lofberg, "Yalmip: A toolbox for modeling and optimization in matlab," in *2004 IEEE international conference on robotics and automation (IEEE Cat. No. 04CH37508)*. IEEE, 2004, pp. 284–289.

[17] "Gurobi optimizer reference manual," Gurobi Optimization, 2021.

[18] L. T. Biegler and V. M. Zavala, "Large-scale nonlinear programming using ipopt: An integrating framework for enterprise-wide dynamic optimization," *Computers & Chemical Engineering*, vol. 33, no. 3, pp. 575–582, 2009.